Interactions of Some Novel Amide-Linked Bis(acridines) with Deoxyribonucleic Acid†

H. Dalton King,‡ W. David Wilson,* and E. J. Gabbay§

ABSTRACT: A novel series of bis(acridines) has been synthesized in which the two potential intercalating chromophores are separated by symmetrical amide-linked chains varying in both length and conformational flexibility. By comparison to a monointercalating adduct, mono- vs. bis-intercalative behavior has been established for the bis(acridines). Spectrophotometric (visible, circular dichroism, and fluorescence) and viscometric (linear sonicated and closed circular superhelical DNA) experiments indicate that a highly rigid 8.8 Å separated bis(acridine) monointercalates, whereas the longer and more flexible bis(acridines) are capable of bis-intercalation. In addition, spectrophotometric studies suggest a correlation between the tendency of intramolecular association and the ability to bis-intercalate. The results are in agreement with predictions based on the neighbor-exclusion principle and indicate that connecting chain rigidity is capable of playing a determining role in the mono- vs. bis-intercalation mechanism.

In an effort to develop more effective chemotherapeutic drugs, many researchers have focused their studies on DNA intercalating drugs that possess enhanced binding affinity and/or sequence selectivity. A prevailing hypothesis is that an increase in DNA binding affinity can be correlated with an increase in medicinal activity. This idea is simplistic at best, since many factors affect biological activity, such as membrane permeability, metabolic degradation, site specificity, and toxic side effects. Despite these factors, there are instances where this correlation has proven to be correct (Wilson & Jones, 1982). As an example of such an approach, bifunctional intercalating drugs have been synthesized and isolated from natural sources (Schock, 1957; Le Pecq et al., 1975; Wakelin et al., 1978; Canellakis et al., 1976; Gaugain et al., 1978; Becker & Dervan, 1979; Kuhlmann et al., 1978; Pelaprat et al., 1980; Wakelin & Waring, 1976; Lee & Waring, 1978; Huang et al., 1980; Viswamitra et al., 1981; Wilson et al., 1982). By connection of two potential intercalating moieties with a molecular chain, a compound can be attained that, in the absence of unfavorable geometric and entropic factors, possesses a high DNA binding constant, approaching the square of that of the comparable monointercalator.

Such compounds are attractive not only for their medicinal properties but also for the structural information concerning the drug–DNA complex that may be obtained. The synthesis of potential bis-intercalators possessing optimal geometric and conformational characteristics has been the goal of several research efforts. A great deal of interest has centered on the nature of the chain connecting the two intercalators. In an attempt to demonstrate bis-intercalation, Le Pecq et al. (1975) studied a series of poly(alkylamine)linked bis(2-methoxy-6-chloro-9-aminoacridines). They found that bis-intercalation occurred for their longer chain adducts in which it was possible to incorporate two base pairs between the bound ligands. The minimum chain length or "interligand distance" corresponding to this separation is 10.2 Å, in agreement with predictions based on the neighbor-exclusion model. Wakelin et al. (1978) examined a series of polyalkyl-linked bis(acridines) and determined that the minimum interligand distance at which bis-intercalation could be observed for these derivatives was around 8.8 Å. If a classical intercalation model holds for these compounds, this distance requires binding of the two ligands at adjacent sites on the DNA lattice, in violation of neighbor exclusion and in contrast to the results of LePecq and coworkers. It has been proposed that the discrepancy in the minimum length for the connector chain to allow bis-intercalation is due to differences in aromatic ring substitution and that the nature of the connecting chain, with the exception of its length, has little effect on the actual mode of intercalation (Wright et al., 1980). Some results have indicated, however, that connecting chain flexibility plays a vital role in the bis-intercalation mechanism (Chen & Whitlock, 1978; Pelaprat et al., 1980; Gaugain et al., 1978; Wilson et al., 1982). A number of studies utilizing nuclear magnetic resonance (NMR) (Gaugain et al., 1978; Roques et al., 1976) and kinetic methods (Chen & Whitlock, 1978) show flexible bis-intercalators to self-associate in solution via stacking of the aromatic bases. Obviously, the unfolding process is a prerequisite for bis-intercalation. It follows then that a rigid connecting chain would disfavor self-association and could facilitate insertion of both ligands into the DNA lattice.

We have synthesized a series of amide-linked bis(acridines) that not only offers increased rigidity due to the amide linkages but also exhibits enhanced water solubility while remaining uncharged. As shown in Table I, the maximum interligand distance for these compounds was varied from 8.8 to 21.6 Å, allowing the examination of compounds capable of spanning from one to five base pairs upon binding. This series has an uncharged connector chain as with the derivatives of Wakelin et al. (1978) but is still polar and, thus, is intermediate in character between the acridines of Wakelin et al. (1978) and the charged connector compounds of Le Pecq et al. (1975). Evaluation of a variety of derivatives of this type is extremely important in determining the structural and/or thermodynamic basis of neighbor-exclusion binding and how this can be violated by some bis-intercalators. The interactions with DNA of the bis(acridines) of Table I, along with similar monoacridines for comparison purposes, have been investigated by spectroscopic and viscometric techniques by utilizing both

† From the Department of Chemistry, University of Florida, Gainesville, Florida 32611 (H.D.K. and E.J.G.), and the Department of Chemistry and Laboratory for Microbial and Biochemical Sciences, Georgia State University, Atlanta, Georgia 30303 (W.D.W.). *Received February 18, 1982.* This research was supported by National Institutes of Health Grants GM 30267 and RR 09201.

‡ Present address: Department of Biology, University of Pennsylvania, Philadelphia, PA 19104.

§ Deceased, 1979.

0006-2960/82/0421-4982$01.25/0

Table I: Structures of the Monoacridines and Bis(acridines)

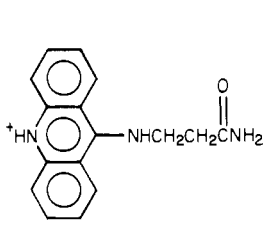

1

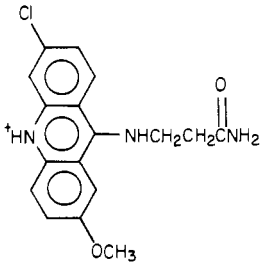

2

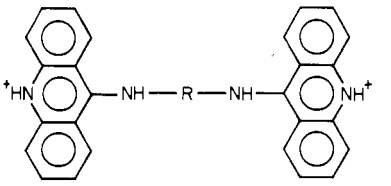

3–6

compd	R for 3–6	interligand distance (Å)[a]
3	$-CH_2C(=O)NHNHC(=O)CH_2-$	8.8
4	$-CH_2CH_2C(=O)NH(CH_2)_2NHC(=O)CH_2CH_2-$	13.2
5	$-CH_2CH_2C(=O)NH(CH_2)_3NHC(=O)CH_2CH_2-$	14.4
6	$-CH_2CH_2C(=O)NHCH_2C(=O)NH(CH_2)_3NHC(=O)CH_2NHC(=O)CH_2CH_2-$	21.6

[a] Interligand distances represent the maximum possible separation of the two acridine chromophores as measured from 9-amino to 9'-amino group of CPK models. In calculation of these values, all bonds have been placed in the totally staggered conformations, resulting in fully extended chains.

linear and closed circular superhelical DNA.

Experimental Procedures

Materials

All starting amino acids were purchased from either Sigma Chemical Co., Aldrich Chemical Co., or Vega Biochemicals. The carbobenzoxy-protected amino acids were supplied by Sigma and all other materials by Aldrich. Unless otherwise noted, all were used without further purification. Elemental analyses were performed by Atlantic Microlab, Inc. Melting points were measured on either a Mel-Temp apparatus or a Thomas Hoover Uni-melt apparatus and are uncorrected. Thin-layer chromatograms were run on 0.2-mm silica gel 60 F_{254} sheets obtained from MC/B Manufacturing Chemists, Inc. The TLC[1] solvent system used was 2% diethylamine–methanol unless otherwise noted. ^1H NMR spectra were obtained in dimethyl-d_6 sulfoxide on either a JEOL JNM-FX-100 Fourier-transform NMR spectrometer or a JEOL JNM-PMX-60 NMR spectrometer. Chemical shifts were determined relative to the internal standard tetramethylsilane.

N-9-Acridinyl-β-alanylamide (**1**). 9-Methoxyacridine (Lehmstedt, 1935) (840 mg, 4.0 mmol) and β-alanylamide hydrochloride (500 mg, 4.0 mmol) were dissolved in 10 mL of methanol and allowed to stand for 2 days (Adcock, 1973). Yellow needles formed, which were filtered and air-dried. Recrystallization was possible only from dimethyl sulfoxide, yielding *N*-9-acridinyl-β-alanylamide hydrochloride (1.05 g, 86.7%) after thorough vacuum drying (100 °C), mp >250 °C dec. TLC showed one spot, R_f 0.40. Anal. Calcd for $C_{16}H_{16}N_3OCl{\cdot}0.5H_2O$: C, 61.84; H, 5.51; N, 13.52. Found: C, 61.92; H, 5.53; N, 13.48.

N-9-(2-Methoxy-6-chloroacridinyl)-β-alanylamide (**2**). Approximately 50 g of phenol was distilled at reduced pressure onto 6,9-dichloro-2-methoxyacridine (15.0 g, 0.0540 mol) and the mixture stirred at 120 °C for 1 h. β-Alanine (5.76 g, 0.0647 mol) was then added and stirring at 120 °C continued for 2 h (Adcock, 1973; Dupre & Robinson, 1945; Organon, 1957). The mixture was cooled until it solidified and then stirred in $H_2O/CHCl_3$, precipitating a yellow solid. This solid was dissolved in 250 mL of 1 N NaOH, filtered, and carefully acidified with glacial acetic acid (Organon, 1957) to give the yellow product. This was filtered and washed with H_2O, 10 mL of methanol, and finally ether. Vacuum drying over P_2O_5 afforded *N*-9-(2-methoxy-6-chloroacridinyl)-β-alanine (12.14 g, 68.0%), mp 230 °C. Anal. Calcd for $C_{17}H_{15}N_2O_3Cl{\cdot}2H_2O$: C, 55.67; H, 5.22. Found: C, 55.63; H, 5.61.

The acridine derivative (2.8 g, 0.0085 mol) was dissolved in anhydrous ethanol saturated with HCl gas at 0 °C and stirred for 2 h. After removal of the solvent, the yellow residue was dissolved in 100 mL of 1 M NaOH/150 mL of ethyl acetate. The organic phase, extracted 3 times with 1 M NaOH and once with H_2O, was dried over magnesium sulfate. The ethyl acetate was evaporated and the yellow-orange solid recrystallized from chloroform, yielding *N*-9-(2-methoxy-6-chloroacridinyl)-β-alanine ethyl ester (1.51 g, 49.4%).

In a high-pressure reaction vessel, the ester (1.43 g, 0.0040 mol) was dissolved in 50 mL of methanol and cooled to −78 °C; then, NH_3 was bubbled into the solution until it was saturated. The vessel was tightly closed and allowed to stand at room temperature for 2 days. Solvents and NH_3 were removed with an N_2 stream. Other solvent systems being unsuitable, dimethyl sulfoxide was used to recrystallize the crude product. Thorough vacuum drying afforded *N*-9-(2-methoxy-6-chloroacridinyl)-β-alanylamide (0.778 g, 59.3%), mp 219–219.6 °C. TLC, methanol as the solvent system, exhibited one spot, R_f 0.38. Anal. Calcd for $C_{17}H_{16}N_3O_2Cl$: C, 61.91; H, 4.89; N, 12.74. Found: C, 61.83; H, 4.88; N, 12.68.

N,N'-Bis(N-9-acridinylglycyl)hydrazine Dihydrobromide (**3**). *N,N'*-Bis(carbobenzoxyglycyl)hydrazine (Rolski & Rolski, 1969) (520 mg, 1.25 mmol) was suspended in 25 mL of 34% HBr/acetic acid and a calcium chloride drying tube used to exclude moisture. The mixture was stirred 1 h, during which time gas was evolved. Excess ether was added to precipitate the crude product, which was filtered under N_2 and reprecipitated from ethanol/ether. The solid was vacuum-dried, yielding *N,N'*-bis(glycyl)hydrazine dihydrobromide (181 mg, 46.8%).

N,N'-Bis(glycyl)hydrazine dihydrobromide (161 mg, 0.523 mmol) was dissolved in 15 mL of methanol/0.8 mL of water.

[1] Abbreviations: TLC, thin-layer chromatography; CCS DNA, closed circular superhelical DNA; CD, circular dichroism; ν, moles of acridine derivative bound per DNA base pair; η, reduced specific viscosity; T_m, midpoint temperature of the thermal denaturation curve for DNA solutions; ϵ_f and ϵ_b, extinction coefficients of acridines in solution and bound to DNA; DMF, dimethylformamide; Me_2SO, dimethyl sulfoxide; CPK, Corey–Pauling–Koltun.

9-Methoxyacridine (220 mg, 1.051 mmol) was added (Adcock, 1973), and within 2 min a thick yellow precipitate formed. The slurry was stirred 20 h. The yellow precipitate was filtered and washed with a small amount of methanol and ether. This solid was recrystallized from 50:50 methanol/H_2O (20 mL) to yield 98 mg of *N,N'*-bis(*N*-9-acridinylglycyl)hydrazine dihydrobromide. The mother liquor was concentrated and cooled, yielding an additional 82 mg of product (total yield 180 mg, 52%), mp >240 °C dec. TLC of the product showed one spot, R_f 0.49. Anal. Calcd for $C_{30}H_{26}N_6O_2Br_2$: C, 54.40; H, 3.96; N, 12.69. Found: C, 54.63; H, 4.00; N, 12.50.

N,N'-Bis(N-9-acridinyl-β-alanyl)-1,2-ethylenediamine (**4**). The syntheses of **4**–**6** were very similar; therefore, only that of **4** is presented in its entirety. Analytical data for **5**, **6**, and their respective intermediates are presented following this section.

Carbobenzoxy-β-alanine (10.0 g, 0.0448 mol) was dissolved in 150 mL of dry tetrahydrofuran. Triethylamine (18.7 mL, 0.135 mol) was added, and stirring maintained for 30 min at 0 °C under an N_2 stream. Isobutyl chloroformate (5.82 mL, 0.0448 mol) was added to form the mixed anhydride (Greenstein & Winitz, 1971). Stirring at 0 °C under N_2 was continued for 1 h, at which time ethylenediamine (98%, 1.53 mL, 0.0224 mol) in 10 mL of dry tetrahydrofuran was added dropwise. The mixture was allowed to warm slowly to room temperature and stirred overnight. Solvents were rotary evaporated to dryness, and the tannish residue was washed successively with H_2O, 0.1 M HCl, H_2O, saturated $NaHCO_3$, and H_2O. The crude white solid was recrystallized from *N,N*-dimethylformamide, yielding after filtration and vacuum drying (60 °C) pure *N,N'*-bis(carbobenzoxy-β-alanyl)-ethylenediamine (3.88 g, 18.4%), mp 187–190 °C. Anal. Calcd for $C_{24}H_{30}N_4O_6 \cdot 0.5H_2O$: C, 60.11; H, 6.52. Found: C, 59.79; H, 6.51.

N,N'-Bis(carbobenzoxy-β-alanyl)ethylenediamine (1.50 g, 3.19 mmol) was suspended in 25 mL of saturated (34%) HBr/acetic acid. The mixture was stirred for 1 h, during which time the evolution of CO_2 gas was observed. Excess ether was added to precipitate the product, which was filtered under N_2. The crude product was dissolved in 5 mL of methanol and excess ether added dropwise to precipitate pure *N,N'*-bis(β-alanyl)-1,2-ethylenediamine dihydrobromide (938 mg, 80.6%), which was filtered under N_2 and vacuum-dried.

N,N'-Bis(β-alanyl)ethylenediamine dihydrobromide (512 mg, 1.41 mmol) and 9-methoxyacridine (619 mg, 2.96 mmol) were heated at approximately 50 °C for 14 h in 50 mL of methanol (Adcock, 1973; Organon, 1957; Barber et al., 1947). Solvents were removed by rotary evaporation. The crude product was purified by elution with 4% diethylamine/methanol on a dry silica gel column. An orange solid was obtained that proved difficult to recrystallize, so it was dissolved in a minimum volume of methanol and precipitated with ether. Filtration of the orange solid under N_2 yielded *N,N'*-bis(*N*-9-acridinyl-β-alanyl)-1,2-ethylenediamine (479 mg, 61.3%), mp 115–120 °C. TLC analysis showed one spot, R_f 0.43. Anal. Calcd for $C_{34}H_{32}N_6O_2 \cdot 1.5H_2O$: C, 69.96; H, 6.04; N, 14.40. Found: C, 70.40; H, 6.07; N, 14.53.

N,N'-Bis(N-9-acridinyl-β-alanyl)-1,3-diaminopropane (**5**). *N,N'*-Bis(carbobenzoxy-β-alanyl)-1,3-diaminopropane was prepared by the mixed-anhydride procedure and recrystallized from DMF (30.0% yield; mp 175–179 °C). Anal. Calcd for $C_{25}H_{32}N_4O_6$: C, 61.97; H, 6.66. Found: C, 61.84; H, 6.75.

Cleavage in HBr-saturated acetic acid yielded *N,N'*-bis(β-alanyl)-1,3-propanediamine dihydrobromide (90.0%). This salt was reacted with 9-methoxyacridine by the established procedure to yield **5**. Silica gel chromatography provided the pure product in 19.7% yield (mp 135 °C dec; R_f 0.43). Anal. Calcd for $C_{35}H_{24}N_6O_2 \cdot 2.3H_2O$: C, 68.68; H, 6.36; N, 13.73. Found: C, 68.61; H, 6.48; N, 14.12.

N,N'-Bis[N-(9-acridinyl-β-alanyl)glycyl]-1,3-diaminopropane (**6**). *N,N'*-Bis[(carbobenzoxy-β-alanyl)glycyl]-1,3-diaminopropane was prepared by the mixed-anhydride procedure and recrystallized from DMF (66.1% yield; mp 225–226 °C). Anal. Calcd for $C_{29}H_{38}N_6O_8$: C, 58.18; H, 6.40. Found: C, 58.08; H, 6.42.

HBr–acetic acid cleavage yielded *N,N'*-bis(β-alanylglycyl)-1,3-propanediamine dihydrobromide (92.7%), which was reacted with 9-methoxyacridine to yield, after chromatographic workup, pure **6** [70.5%; mp 140 °C dec; R_f 0.41]. Anal. Calcd for $C_{39}H_{40}N_8O_4 \cdot 3H_2O$: C, 63.40; H, 6.28; N, 15.17. Found: C, 63.33; H, 6.31; N, 15.13.

Sonicated calf thymus DNA (Worthington Biochemical Co.) was prepared as previously reported (Jones et al., 1980). By an electrophoretic method (Jones et al., 1980), its molecular weight was determined to be 800000–900000. Concentrations of stock solutions were determined spectrophotometrically by using an extinction coefficient of 6500 at 258 nm (Chargraff et al., 1951). Closed circular superhelical Col E1 plasmid DNA was prepared as previously described (Jones et al., 1980).

All drug and DNA solutions were prepared in buffers made with distilled deionized water. Mes_{00} buffer is 1.0×10^{-2} M 2-(*N*-morpholino)ethanesulfonic acid (Mes), 1.0×10^{-4} M ethylenediaminetetraacetic acid (EDTA), and 5×10^{-3} M Na^+, pH 6.2. Mes_{10} buffer is 1.0×10^{-2} M Mes, 1.0×10^{-4} M EDTA, and 0.105 M Na^+, pH 6.2. $Pipes_{00}$ buffer is 1.0×10^{-2} M 1,4-piperazinediethanesulfonic acid (Pipes) and 1.0×10^{-3} M EDTA, pH 7.0.

Drug stock solutions were prepared by carefully weighing appropriate quantities of the solid compounds into dry 2-mL volumetric flasks and dissolving in buffer to obtain concentrations of $(1–2) \times 10^{-3}$ M. The following buffer systems were used for each stock solution: **1** and **2**, 0.025 M lactic acid–Mes_{00}; **3**, 20% Me_2SO–Mes_{00}; **4**–**6**, Mes_{00}.

Methods

Viscosity Studies. Linear- and CCS-DNA viscometric titrations were performed in Series 75 Cannon-Ubbelohde semimicrodilution viscometers (Cannon Instrument Co.). Temperature was maintained at 25 ± 0.01 °C in a thermostated water bath. Flow times were electronically measured by a Wescan fiber optic detection unit and timer (Wescan Instrument Co.).

In a typical experiment (Jones et al., 1979), flow times for the buffer, DNA solution, and DNA–drug complex (at varying *r* values) were measured. At least two trials were made for each measurement, and if times did not agree within 0.05 s, the process was repeated until sufficient agreement was attained. All solutions were filtered through 0.22-μm Millipore filters prior to viscometric measurements.

Circular Dichroism Studies. CD experiments were conducted at ambient temperature in a Jasco J-500C spectropolarimeter. Two different approaches were taken: In the first, small aliquots of a concentrated drug solution (1×10^{-3} M) were added to a dilute DNA solution (3×10^{-4} M) in the appropriate buffer in a 5-cm cell. The spectrum, after each addition, was recorded from 500 to 300 nm. Drug additions were made until no further changes in the spectrum were seen. In the second approach, a concentrated DNA solution (6.2×10^{-2} M) was added to the drug dissolved in the appropriate buffer (2×10^{-5} M) in a 5-cm cell and the spectrum recorded as before.

Table II: Spectroscopic Data for 1 and 3-6[a]

	visible absorption					fluorescence emission		circular dichroism[g]	
	free		bound			free	bound		
compd	λ_{max} (nm)	ϵ_f[b]	λ_{max} (nm)	ϵ_b[c]	% H[d]	λ_{max} (nm)[e]	λ_{max} (nm)[f]	$[\theta]_{329} \times 10^{-3}$[h]	$[\theta]_{417} \times 10^{-3}$
1	412	11 300	416	5 560	103.2	415 (sh), 442	415, 442	7.9	0.75
3	412	21 700	414	12 200	78.6	415, 442	415, 439	1.5	14
4	412	16 400	416	9430	74.0	416, 439	416, 439	16	−4.1
5	412	16 500	416	9 960	65.7	415, 438	415, 438	17	−5.4
6	412	16 800	416	10 600	57.9	416, 438	416, 438	18	−4.4

[a] All other experiments were conducted in Mes_{10} buffer at 25 °C. [b] Extinction coefficients of the free compound in the absence of DNA at 412 nm. Units are liters per centimeter per mole. [c] Extinction coefficient of the fully bound compound in the presence of excess calf thymus DNA at 412 nm; compound/DNA-P ratio ≤0.01. [d] Percent hypochromicity, % $H = (\epsilon_f/\epsilon_b - 1) \times 100$. [e] Emission maxima of the acridine (2.1×10^{-6} M) in the absence of calf thymus DNA. Excitation was at 390 nm. [f] Emission maxima of the acridine (2.1×10^{-6} M) in the presence of excess calf thymus DNA (drug/DNA-P ratio ≤0.002). Excitation was at 390 nm. [g] Acridine solutions were titrated with con concentrated DNA solution to a compound/DNA-P ratio of 0.03, in a 5-cm cell. Acridine concentrations were approximately 2×10^{-5} M, except 3 whose concentration was 1×10^{-5} M. [h] Molar ellipticity is defined as $[\theta] = M\Psi/(100lC)$ where M is the molecular weight of the acridine derivative, Ψ is molecular ellipticity in degrees, l is the cell path length in decimeter, and C is the drug concentration grams per milliliter. The units for $[\theta]$ are degrees centimeter squared per decimole.

Fluorescence Studies. All fluorescence spectra were measured in Perkin-Elmer MPF-44A spectrofluorometer and are uncorrected. Initially, the emission spectrum of a dilute drug solution (2×10^{-6} M) was obtained from 360 to 650 nm (excitation at 390 nm). A concentrated calf thymus DNA solution (6.2×10^{-3} M) was then added in small aliquots, and the spectrum was recorded after each addition. DNA was added until the drug/DNA-P ratio had decreased to 0.002 or lower. The change in emission intensity relative to the original signal ($\Delta F/F_1$) at the emission maximum was calculated and plotted vs. DNA concentration.

Absorption Studies. Absorption spectra (500–320 nm) were obtained from either a Cary-17D or a Cary 219 UV–vis spectrophotometer at ambient temperature. The extinction coefficient of the free drug (ϵ_f) was obtained by titrating a drug stock solution into either a 1- or 10-cm cell containing the appropriate buffer and relating the observed maximum absorbance to concentration according to Beer's law by linear regression analysis. To avoid deviations from ideal Beer's law behavior, we kept concentrations of the monoacridines below 1×10^{-5} M and those of the bis(acridines) below 6×10^{-6} M. The extinction coefficient of the DNA–drug complex (ϵ_b) was determined by an identical procedure, except that the drug was titrated into a concentrated DNA solution (6×10^{-3} M). Absorbances were read at the same wavelength as for the calculation of ϵ_f. In both cases, linear plots with correlation coefficients of 0.9999 or better were obtained at these low concentrations. Percent hypochromicity (% H) was calculated from

$$\% H = (1 - \epsilon_f/\epsilon_b) \times 100 \quad (1)$$

Melting Temperature (T_m) Studies. DNA melting temperatures were measured in 1-cm quartz cells in a Cary 219 spectrophotometer equipped with automatic recording accessories. The cell holder was thermostated with a Neslab EX-100 constant temperature bath and the temperature regulated with a Neslab ETP-3 temperature programmer. Heating rates of 0.5 °C/min were used.

Drug–DNA complexes were prepared by adding sufficient drug stock solution to 4.9×10^{-5} M calf thymus DNA in $Pipes_{00}$ buffer to obtain a drug/DNA-P ratio of 0.050 for monoacridines **1** and **2** and 0.025 for bis(acridines) **3–6**.

Results

Before discussing the interactions of **1–6** with DNA, it is informative to examine the geometrical and conformational characteristics of the bis(acridines). By use of space-filling CPK models, the interligand distance as well as the overall degree of chain rigidity can be estimated. Table I lists the structures of **1–6** and the corresponding N–N interligand distances. The N–N distances were also calculated from standard bond lengths and angles, and as has been found by others (Wakelin et al., 1978), the agreement with the measurements from CPK models was excellent. It should be emphasized that in calculation of this separation by both methods, the linking chains were placed in a totally staggered conformation; therefore, these estimates represent the maximum length. In the case of **3**, such an arrangement leaves the connecting chain in a very inflexible conformation in which fluctuations are minimized because of severe steric strain. However, despite their amide linkages, the longer bis(acridines) **4–6** have considerable conformational flexibility and are able to fold into a broad range of conformations. It can be predicted, then, that **4–6** are capable of classical bis-intercalation intercalation since the interligand distance is long enough (>10.2 Å) to allow binding site exclusion and there are no conformational constraints to prevent bis-intercalation. On the other hand, an accurate prediction for **3** is more difficult since its interligand distance (8.8 Å) will allow bis-intercalation only at adjacent binding sites or with neighbor exclusion if the DNA conformation is distorted.

Spectrophotometric data for **1** and **3–6** are summarized in Table II. By comparing the ϵ_f values for bis(acridines) **3–6** to monoacridine **1**, it is seen that the more flexible **4–6** exhibit significant hypochroism. This is consistent with intramolecular stacking of the chromophores in these compounds (Ts'o, 1968; Chen & Whitlock, 1978; Gaugain et al., 1978; Roques et al., 1976). On the other hand, the more rigid **3** shows little or no evidence of such self-association on the basis of its much larger value of ϵ_f. These observations are in agreement with the predictions based on model building. In comparing the DNA-bound spectrophotometric results, it is interesting to note that while all the monoacridines and bis(acridines) showed the typical spectral shifts associated with intercalation; **3** demonstrates neither as large a red shift nor as large a hypochromic effect as its longer counterparts **4–6**.

This series of monoacridines and bis(acridines) is moderately fluorescent. Upon addition of calf thymus DNA, the fluorescence is strongly quenched, indicating possible intercalative interactions between the chromophores and DNA. Figure 1 shows a representative example of the emission spectra from 400 to 600 nm of the compounds of this series in the presence of an increasing concentration of calf thymus DNA (excitation at 390 nm).

Table III: Physical Constants Characterizing the Interaction of 1–6 with DNA

compd	slope[a]	ϕ (degrees)[d]	r'	C_f (M)[e]	K (M^{-1})[f]	T_m (°C)[g]	ΔT_m (°C)[h]
1	1.6	16	0.082	8.0×10^{-6}	1.9×10^4	71.6	2.8
2	1.6	19	0.068	2.4×10^{-6}	4.6×10^4	71.7	2.9
3	0.8,[b] 1.1[c]	13	0.097	$<10^{-7}$	$>10^6$	73.5	4.7
4	2.5	30	0.044	$<10^{-7}$	$>10^6$	74.0	>5.2
5	2.1	30	0.043	$<10^{-7}$	$>10^6$	>76.6	>7.8
6	3.1	35	0.037	$<10^{-7}$	$>10^6$	>76.6	>7.8

[a] Slopes were calculated by least-squares analysis according to data from Figure 4. [b] Slope of lower region of plot (Figure 4). [c] Slope of upper region of plot (Figure 4). [d] Unwinding angles are based on a value of 26° for ethidium bromide; r' for ethidium bromide was determined to be 0.050 under these conditions. [e] Concentration of unbound drug at the equivalence point of the CCS DNA titration (Figure 6). [f] Estimated DNA binding constant (see text for details). [g] The experiment was conducted in $Pipes_{00}$ buffer, the total ligand/DNA-P ratio was 0.050, and the DNA concentration was 4.94×10^{-5} M phosphate/L. [h] The T_m of calf thymus DNA in the absence of 1–6 was 68.8 °C. ΔT_m is defined as the difference between the T_m of the drug–DNA complex and the T_m of DNA. Curves for compounds 4–6 were biphasic, and the T_m cannot be accurately defined under these conditions.

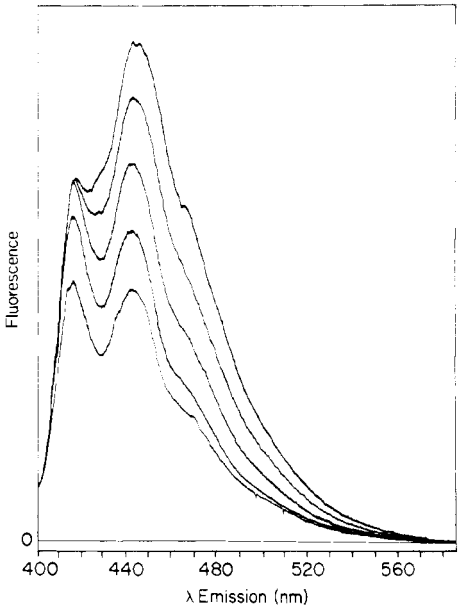

FIGURE 1: Fluorescence emission spectrum of **1** (2.18 μM) in the absence (uppermost curve) and in the presence of increasing concentration of calf thymus DNA. Reading down from the second curve, the drug/DNA-P ratios are 0.11, 0.027, 0.0056, and 0.0018. Excitation was at 390 nm. Each spectrum was obtained in Mes_{10} buffer at ambient temperature in 1-cm quartz fluorescence cuvettes. The behavior of **1** is typical of the remaining members of the series.

Further spectroscopic comparisons of binding are obtained from CD studies. Each member of the series is optically inactive and therefore exhibits no CD spectrum. However, in the presence of calf thymus DNA, a large CD signal is induced in the region 300–500 nm for each acridine. Figure 2 shows several representative spectra. It is interesting to note the overall similarities between the induced CD spectra of **1** and **4**, in marked contrast to that of **3**. Though it is difficult to describe the exact characteristics of the DNA–drug complex from the CD alone, some general comments can be made. By virtue of their common positive CD band at 329 nm (Table II), **1** and **4–6** likely possess very similar DNA-bound structures. The short bis(acridine) **3**, on the other hand, obviously possesses a DNA-bound structure differing from the remainder of the series.

The most graphic evidence of intercalation is supplied by the viscometric behavior of linear sonicated DNA and closed circular superhelical DNA in the presence of drug. Upon intercalation, the base pairs at the binding site unwind, and the helical length is increased by approximately 3.4 Å (Lerman, 1961, 1963, 1964a,b). The lengthening results in an increase in the viscosity of the linear DNA complex. The approximate relationship between viscosity and helix lengthening is given by

$$L_1/L_0 = (\eta_1/\eta_0)^{1/3} = 1 + 2r \qquad (2)$$

where the subscript 1 refers to the DNA complex, the subscript 0 refers to uncomplexed DNA, L is the DNA contour length, η is the reduced specific viscosity, and r is the ratio of bound drug to DNA phosphate. From this equation, a plot of $(\eta_1/\eta_0)^{1/3}$ vs. r will yield a line with slope equal to 2 for an ideal monointercalator. Nonideal behavior is usually observed, with slopes less than 2 being the norm. A bis-intercalator, by this treatment, should exhibit slopes approximately double these of its monointercalating counterpart. Again nonideal behavior results in somewhat lower values (Cohen & Eisenberg, 1969; Pelaprat et al., 1980).

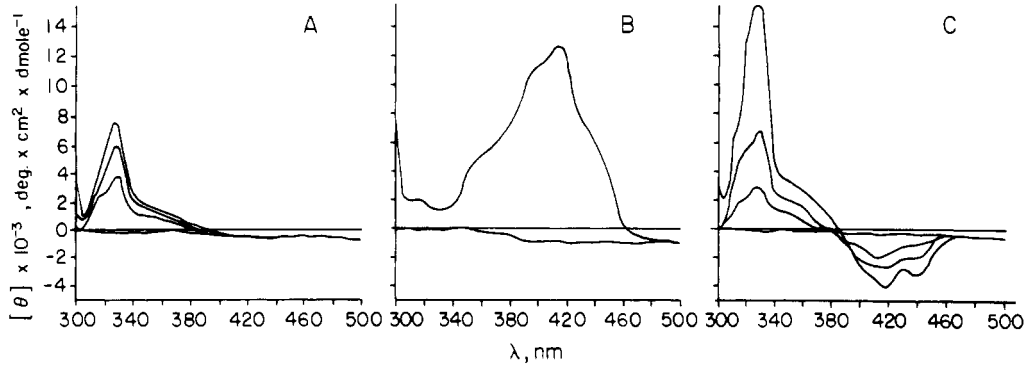

FIGURE 2: CD spectra of some representative acridines in the absence and in the presence of increasing concentration of calf thymus DNA. (A) **1** (22 μM): The base line is the spectrum in the absence of DNA; reading upward, drug/DNA-P ratios are 0.200, 0.099, and 0.033. (B) **3** (11 μM): base line, no DNA; reading upward, drug/DNA-P ratios are 0.083 and 0.025 (both curves superimposed). (C) **4** (25 μM): base line, no DNA; reading upward, drug/DNA-P ratios are 0.571, 0.228, and 0.029. All spectra were obtained in 5-cm cells at ambient temperature in Mes_{10} buffer.

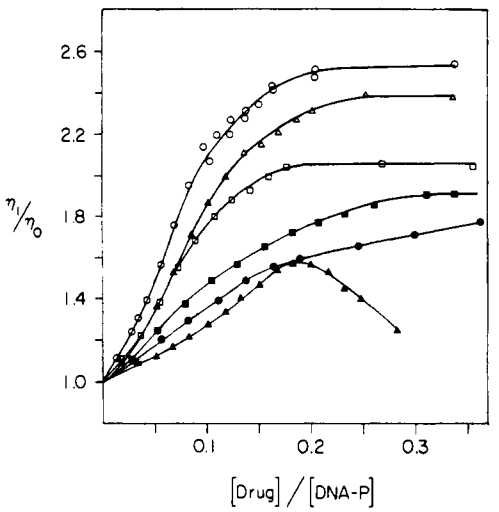

FIGURE 3: Viscometric titrations of sonicated calf thymus DNA with **1** (●), **2** (■), **3** (▲), **4** (△), **5** (□), and **6** (○). The DNA concentration was 0.384 mM phosphate/L. Experiments were carried out in Mes_{10} buffer at 25 °C. Curves for **1** and **2** are uncorrected for unbound drug concentration.

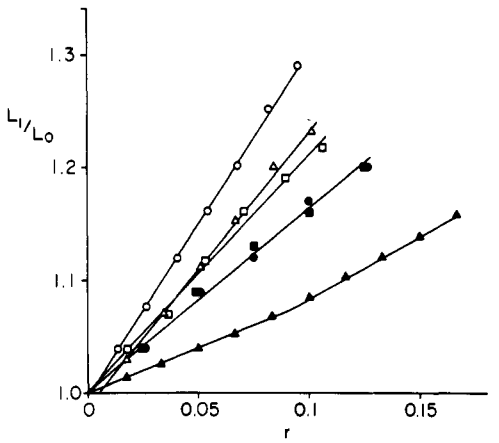

FIGURE 4: Length increase of sonicated calf thymus DNA by **1** (●), **2** (■), **3** (▲), **4** (△), **5** (□), and **6** (○). The results from Figure 3 are plotted according to eq 2. Results for **1** and **2** are corrected for unbound drug concentration by using the K value in Table III. Since bis-intercalation would be expected to saturate at an acridine to DNA ratio of 0.125, no points above that ratio from Figure 3 were used for these compounds in plotting Figure 4.

Figure 3 illustrates the viscometric titrations of linear calf thymus DNA with **1**–**6**. All of the compounds increase the viscosity and, therefore, the length of DNA. Furthermore, a quantitative analysis of these data by eq 2 (Figure 4, Table III) shows that the magnitude of the length increase is significantly larger for bis(acridines) **4**–**6** than for monoacridines **1** and **2**. Though nonideal values are noted for these slopes, the range of values is well within the expected limits. Bis(acridine) **3** presents quite different viscometric behavior. Note that the viscosity profile for **3** in Figure 3 follows an altogether different contour, peaking at a molar ratio value of 0.18 before rapidly falling off. The viscosity decrease is most likely due to the formation of aggregates, as was evidenced by the appearance of a precipitate at highest molar ratios. It is obvious that **3** fails to lengthen DNA to as great an extent as the longer bis(acridines) or even the monoacridines.

The interactions of CCS DNA with **1**–**6** were also studied by viscometry. Figure 5 illustrates several examples of this approach. In its native form, CCS DNA exists in a compact, right-handed superhelical structure. As drug intercalates into the helix, the base pairs unwind, and subsequently, the righthanded supercoils are gradually removed. This process

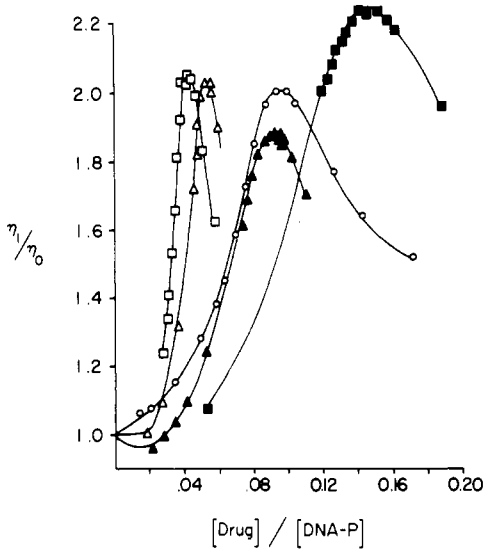

FIGURE 5: Viscometric titrations of closed circular superhelical DNA with **1** (■), **2** (○), **3** (▲), **4** (□), and ethidium bromide (△). DNA concentrations were as follows: **1**, 0.121 mM; **2**, 0.0782 mM; **3**, 0.161 mM; **4**, 0.161 mM; ethidium bromide, 0.16 mM. All experiments were conducted at 25 °C in Mes_{10} buffer.

continues until a point is reached where enough drug is bound to completely remove all the supercoils, resulting in uncoiled closed circular DNA in its fully extended form. Further intercalation of drug past this point will cause continued unwinding of the double helix and supercoiling in the reverse (left-handed) direction. The uncoiled form of closed circular DNA exhibits the highest intrinsic viscosity. From Figure 5, it is seen that **1**–**6** each remove the right-handed supercoils of CCS DNA and then subsequently induce formation of a left-handed superhelical structure. The maximum values of η_1/η_0 in Figure 5 are quite close for all of the compounds. Compound **3** has the lowest η_1/η_0 maximum value, and this agrees with its low L_1/L_0 slope from Figure 4. The reason for the higher L_1/L_0 value for **1**, however, is not obvious since this compound gives an L_1/L_0 slope with linear DNA similar to that for **2**.

The magnitude of helix unwinding can be determined by the method of Vinograd and co-workers (Revet et al., 1971; Jones et al., 1980). The assumption must be made that the amount of bound drug per nucleotide, r', required to completely remove all supercoils is constant at varying DNA concentrations. The quantity r' is related to experimentally measurable quantities by

$$C_t' = r'N_t' + C_f' \quad (3)$$

where C_t' is the total ligand concentration, N_t' is the total nucleic acid concentration, and C_f' is the concentration of unbound drug, all at the intrinsic viscosity maximum. If titrations are conducted at several different concentrations of CCS DNA, a plot of C_t' vs. N_t' can be made in which a straight line with slope r' and ordinate intercept C_f' is obtained. The unwinding angle of a ligand can thus be determined from eq 4, where ϕ_e and ϕ are the unwinding angles for ethidium

$$r_e'\phi_e = r'\phi \quad (4)$$

bromide (26°) (Revet et al., 1971) and the unknown ligand, respectively. The quantity r_e' is determined for ethidium bromide under the same conditions as for that of the unknown.

The results of this analysis are illustrated in Figure 6 and summarized in Table III. Monoacridines **1** and **2** unwind DNA by 16° and 19°, respectively, in close agreement with other similarly substituted acridines (Wilson & Jones, 1982).

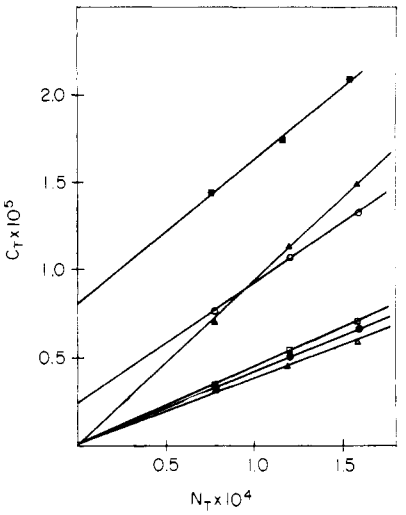

FIGURE 6: Vinograd plot of **1–6**. Viscometric titrations of **1** (■), **2** (○), **3** (▲), **4** (□), **5** (●), and **6** (△) are plotted as total drug concentration (C_t) vs. total DNA concentration (N_t).

A bis-intercalator is expected to generally exhibit unwinding approximately twice the magnitude of the monointercalating counterpart. This is indeed the case for **4–6**, whose values average 32°. Once again, **3** displays characteristics more similar to monoacridines despite its bifunctionality.

In the present study, a determination of equilibrium binding constants by classical methods has not been completed because of the apparent high binding affinity of bis-intercalators and their tendency to stack in solution. Estimates of binding affinity can be made on the basis of the results from Figure 6. Analysis of equilibrium binding data using a site exclusion model can be carried out with

$$r'/C_f = K(1 - 4r')^2/(1 - 2r') \quad (5)$$

where K is the equilibrium binding constant (Bauer & Vinograd, 1970; McGhee & Von Hippel, 1974). If r' and C_f from Figure 6 are used, K can be appoximated for the binding of the drug to CCS DNA (Table III). In the case of **1** and **2**, relatively weak binding constants of 1.3×10^4 M^{-1} and 3.6×10^4 M^{-1} are obtained. However, in the case of **3–6**, very small values of C_f are obtained ($C_f < 10^{-7}$ M), indicating that all the bis(acridines) have extremely large binding constants ($>10^6$ M^{-1}). This result is expected for bis-intercalators such as **4–6** but is rather surprising for the apparent monointercalator **3**. The apparent additional binding affinity of **3** compared to that of **1** is likely due to electrostatic interactions of the nonintercalated aromatic ring with DNA phosphates and perhaps with base pairs protruding into the grooves of the double helix.

Trends in DNA binding affinity may also be obtained from DNA melting temperature experiments. As evidenced by their rather large ΔT_m values (Table III), **1–6** all bind to and stabilize DNA. Only **1** and **2** demonstrate simple, monophasic melting curves in contrast to **3–6**, which exhibit more complicated biphasic melting. Because of the biphasic melting and the high melting temperature of the upper phase, it is not possible to present a simple T_m for **3–6**. It is obvious from these results that the order of increasing DNA affinity is **1**, **2** < **3** < **4**, **5**, **6**.

Discussion

The above results establish unequivocally that **1–6** intercalate between DNA base pairs. Each acridine, in the presence of DNA, exhibits the following spectroscopic evidence: (i) hypochromic and red shifts in the visible spectrum, (ii) quenching of the fluorescence emission spectrum, and (iii) an induced CD spectrum. Additionally, each of **1–6** demonstrates the ability to both lengthen and unwind DNA. Though the spectroscopic results are only suggestive of the bifunctional mode, the viscometric studies, summarized in Table III, verify that **4–6** are bis-intercalators.

The case of bis(acridine) **3** is especially interesting. This compound fails to demonstrate either DNA lengthening or unwinding to as large an extent as even monoacridine **1**. In light of this and the spectroscopic results, **3** must be considered a monointercalator. The apparent deviations of **3** from classical monointercalative behavior are probably due to the presence of its nonintercalated acridine ring in the grooves of the double helix. Interactions of this cationic ring system with DNA phosphates and base pairs and with other nonintercalated rings lead to a smaller degree of helix lengthening and reduced base pair unwinding. The observed increase in DNA binding affinity for **3** relative to those of monointercalators can be correlated to such interactions.

It is interesting to compare the monointercalative behavior of **3** with similar bis(9-aminoacridine) derivatives (Wakelin et al., 1978; Wright et al., 1980). It was concluded by these workers that the results for bis(9-aminoacridine) compounds in the same length range as **3** were consistent with bis-intercalation at adjacent binding sites. Our more rigid compound, **3**, is by all means a monointercalator. Since the major difference between the two systems is the degree of conformational flexibility, we conclude that the increased chain rigidity of **3** does not allow the necessary folding to insert both rings. Thus, **3** represents the first example of a potential bifunctional intercalator inhibited by the linking chain to monointercalation. It is the only unsubstituted bis(9-aminoacridine) derivative that is long enough to bind at adjacent base pairs but that does not do so. The longer adducts, **4–6**, having neither conformational nor geometrical constraints, bis-intercalate as expected.

References

Adcock, B. (1973) in *Heterocyclic Chemistry, Acridines* (Acheson, R. M., Ed.) pp 109–140, Wiley, New York.
Barber, H. J., Wilkinson, J. H., & Edwards, W. G. H. (1947) *J. Soc. Chem. Ind., London 66*, 41.
Bauer, W., & Vinograd, J. (1970) *J. Mol. Biol. 47*, 419.
Becker, M. M., & Dervan, P. (1979) *J. Am. Chem. Soc. 101*, 3664.
Canellakis, E. S., Shaw, Y. H., Hanners, Y. E., & Schwartz, R. A. (1976) *Biochim. Biophys. Acta 418*, 277.
Chargraff, E., Lipschitz, R., Green, C., & Hodes, M. E. (1951) *J. Mol. Biol. 192*, 223.
Chen, C. W., & Whitlock, H. W. (1978) *J. Am. Chem. Soc. 100*, 4921.
Cohen, G., & Eisenberg, H. (1969) *Biopolymers 8*, 45.
Dupre, D. J. & Robinson, F. A. (1945) *J. Chem. Soc.*, 549.
Gaugain, B., Barbet, J., Oberlin, R., Roques, B. P., & Le Pecq, J. B. (1978) *Biochemistry 17*, 5071.
Greenstein, J. P., & Winitz, M. (1971) *Chemistry of the Amino Acids*, p 970, Wiley, New York.
Huang, C. H., Mong, S., & Crooke, S. T. (1980) *Biochemistry 19*, 5537.
Jones, R. L., Davidson, M. W., & Wilson, W. D. (1979) *Biochim. Biophys. Acta 561*, 77.
Jones, R. L., Lanier, A. L., Keel, R. A., & Wilson, W. D. (1980) *Nucleic Acids Res. 8*, 1613.
Kuhlmann, K. F., Charbeneau, N. J., & Mosher, C. W. (1978) *Nucleic Acids Res. 5*, 2629.
Lee, J. S., & Waring, M. J. (1978) *Biochem. J. 173*, 115.
Lehmstedt, K. (1935) *Chem. Ber. 68*, 1455.

Le Pecq, J. B., Le Bret, M., Barbet, J., & Roques, R. (1975) *Proc. Natl. Acad. Sci. U.S.A. 72*, 2915.
Lerman, L. S. (1961) *J. Mol. Biol. 3*, 18.
Lerman, L. S. (1963) *Proc. Natl. Acad. Sci U.S.A. 49*, 94.
Lerman, L. S. (1964a) *J. Cell. Comp. Physiol. 64 (1)*, 1.
Lerman, L. S. (1964b) *J. Mol. Biol. 10*, 367.
McGhee, J. D., & von Hippel, P. H. (1974) *J. Mol. Biol. 86*, 469.
Organon, N. V. (1957) Dutch Patent 83956.
Pelaprat, D., Delbarre, A., Le Guen, I., Roques, B. P., & Le Pecq, J. B. (1980) *J. Med. Chem. 23*, 1336.
Revet, B. M. J., Schmir, M., & Vinograd, J. (1971) *Nature (London), New Biol. 229*, 10.
Rolski, S., & Rolski, K. (1969) *Acta Pol. Pharm. 26*, 301.
Roques, B. P., Barbet, J., & Le Pecq, J. B. (1976) *C. R. Hebd. Seances Acad. Sci. Ser. D 283*, 1453.
Schock, R. U. (1957) *J. Am. Chem. Soc. 79*, 1672.
Ts'o, P. O. P. (1968) in *Molecular Associations in Biology* (Pullmann, B., Ed.) Academic Press, New York.
Viswamitra, M. A., Kennard, O., Cruse, W. B. T., Egert, E., Sheldrick, G. M., Jones, P. G., Waring, M. J., Wakelin, L. P. G., & Olsen, R. K. (1981) *Nature (London) 289*, 817.
Wakelin, L. P. G., & Waring, M. J. (1976) *Biochem. J. 157*, 721.
Wakelin, L. P. G., Romanos, M., Chen, T. K., Glaubiger, D., Canellakis, E. S., & Waring, M. J. (1978) *Biochemistry 17*, 5057.
Wilson, W. D., & Jones, R. L. (1982) in *Intercalation Chemistry* (Whittingham, S., Ed.) pp 177–222, Academic Press, New York.
Wilson, W. D., Keel, R. A., Jones, R. L., & Mosher, C. W. (1982) *Nucleic Acids Res. 10*, 4093.
Wright, R. G., Wakelin, L. P. G., Fields, A., Acheson, R. M., & Waring, M. J. (1980) *Biochemistry 19*, 5825.

Anion Binding and pH-Dependent Electrostatic Effects in Ribonuclease†

James B. Matthew and Frederic M. Richards*

ABSTRACT: The solvent-accessibility-modified, Tanford–Kirkwood, discrete charge model for electrostatic effects is applied to both ribonuclease A and ribonuclease S. The behavior of individual titratable sites and the pH-dependent free energy of denaturation are correctly predicted. The use of the solvent-accessibility factor in reducing charge-site interactions introduces a higher Coulombic shielding for solvent-exposed sites. This shielding is interpreted as a higher local strength or alternatively a higher effective dielectric constant. Specific anion binding sites are determined by locating areas of high positive electrostatic potential at the protein solvent interface. The potential and thus the anion affinity of a given site are calculated and shown to vary with the pH-dependent charge array. pH-dependent anion binding constants are calculated for the ribonuclease S active site. These binding constants and the predicted response of the active-site histidine p$K_{1/2}$ values to anion binding are shown to agree with experimental determinations.

The Tanford–Kirkwood discrete charge theory for globular proteins describes the calculation of an interaction energy between two point charges separated from each other by a distance, r_{ij}, on, or in, a sphere of low dielectric constant surrounded by a solvent of higher dielectric constant with a finite ionic strength. The latter appearance of detailed protein structures from X-ray diffraction studies provided positions for the charged groups and thus removed the ad hoc assumptions about position which had been required in the early work. However, Tanford & Roxby (1972) abandoned the dielectric sphere model as a predictive tool when they determined that an adjustable burial parameter was required to fit protein titration curves. In an attempt to overcome the uncertainty of the burial parameter and to allow for the irregularities of the protein surface, Shire et al. (1974) introduced a modification where the single burial parameter was replaced by the fractional solvent accessibility of each ionizable group as determined from crystal structural data. The development of this general procedure and the current algorithms in use are reviewed (Matthew et al., 1979a, 1981b).

To date, the static-accessibility-modified, Tanford–Kirkwood, theory has been successfully applied to sperm whale myoglobin and 11 species variations (Botelho et al., 1978; Friend & Gurd, 1979a,b), to oxy- and deoxyhemoglobins and their interactions involving hydrogen ions, chloride ions, carbamino adducts, and organic phosphate polyanions (Matthew et al., 1979a,b, 1981a,b), and to protein–protein interactions (Friend et al., 1981). The intent of these studies has been to test the versatility and predictive power of the algorithm by treating a variety of proteins. The mathematical detail (Matthew et al., 1979a), the sensitivity to variations in model parameters (Matthew et al., 1978, 1979a), and the effects of charge array dissymmetries with respect to charge conformation and static solvent accessibility (Matthew et al., 1979b) have been examined.

In this paper we examine the influence of the static-accessibility parameters on the Tanford–Kirkwood work factors. The actual insertion of charged groups into the bulk solvent, as reflected by increased accessibility, results in a set of reduced interaction energies. These reduced pair interactions are interpreted either as a higher effective dielectric constant which includes the bulk ionic strength value or as a higher local ionic strength in the bulk dielectric medium.

Using the calculated protein charge array and the known protein surface topography, we develop a procedure for the identification of specific ion binding sites at the protein surface

† From the Department of Molecular Biophysics and Biochemistry, Yale University, New Haven, Connecticut 06511. *Received December 8, 1981; revised manuscript received April 14, 1982.* This work was supported by National Institute of General Medical Sciences Grant GM-22778. J.B.M. was supported by Fellowship F32 CA06633 from the National Cancer Institute.

0006-2960/82/0421-4989$01.25/0